The role of pressure anisotropy on the maximum mass of cold compact stars

S KARMAKAR[1], S MUKHERJEE[2], R SHARMA[3] and S D MAHARAJ[3]

[1]Department of Physics, North Bengal University, Darjeeling 734 430, India
[2]Inter-University Centre for Astronomy and Astrophysics, Post Bag 4, Ganeshkhind,
Pune 411 007, India
[3]Astrophysics and Cosmology Research Unit, School of Mathematical Sciences, University
of KwaZulu-Natal, Private Bag X54001, Durban 4000, South Africa
E-mail: karma@iucaa.ernet.in; sailom@iucaa.ernet.in; 206526115@ukzn.ac.za;
maharaj@ukzn.ac.za.

Abstract. We study the physical features of a class of exact solutions for cold compact anisotropic stars. The effect of pressure anisotropy on the maximum mass and surface red-shift is analysed in the Vaidya–Tikekar model. It is shown that maximum compactness, red-shift and mass increase in the presence of anisotropic pressures; numerical values are generated which are in agreement with observation.

Keywords. Compact stars; maximum mass; surface red-shift.

PACS Nos 95.30.Sf; 04.20.-q; 04.20.Jb

1. Introduction

The description of very compact astrophysical objects has been a key issue in relativistic astrophysics for the past decades. Recent observations suggest that there are many compact objects such as X-ray pulsar Her X-1, X-ray burster 4U 1820-30, millisecond pulsar SAX J 1808.4-3658, X-ray sources 4U 1728-34, PSR 0943+10 and RX J185635-3754, whose estimated masses and radii are not compatible with the standard neutron star models. The conjecture that quark matter might be the true ground state of hadrons [1,2], inspired many authors to describe such stars as strange stars [3,4], quark–diquark stars [5], hybrid stars [6] and boson/boson–fermion stars [7–11].

As densities of such compact objects are normally above nuclear matter density, theoretical studies suggest that pressures within such stars are likely to be anisotropic, i.e., at the interior of such stars there are two different kinds of pressures, viz., the radial pressure and the tangential pressure [12]. Different solutions

of Einstein's field equations for anisotropic fluid distribution with spheroidal geometry, with varying forms of the energy density, have been obtained by many workers [13–16]. So far, the role of pressure anisotropy has been extensively studied in the context of high red-shift values and stability of compact objects (see for example [17–19] and references therein). Bowers and Liang [20] have pointed out that anisotropy may also change the limiting values of the maximum mass of compact stars. The objective of the present work is to investigate the role of pressure anisotropy on the maximum masses of compact objects. To this end, in §2, we modify a solution obtained by Mukherjee *et al* [21] to incorporate anisotropy. The class of solutions, capable of describing cold compact stars, was obtained by using an ansatz given by Vaidya and Tikekar [22]. For physically relevant anisotropic stars, the regularity and matching conditions for the solutions are developed. In §3 we discuss the role of anisotropy and calculate the maximum possible masses for this class of solutions in §4. We conclude by summarizing our results in §5.

2. Anisotropic model

We take the line element for a static spherically symmetric cold compact star in the standard form

$$\mathrm{d}s^2 = -\mathrm{e}^{2\gamma(r)}\mathrm{d}t^2 + \mathrm{e}^{2\mu(r)}\mathrm{d}r^2 + r^2(\mathrm{d}\theta^2 + \sin^2\theta\mathrm{d}\phi^2), \tag{1}$$

where $\gamma(r)$ and $\mu(r)$ are the two unknown metric functions. Assuming the energy momentum tensor for an anisotropic star in the most general form

$$T_{ij} = \mathrm{diag}\ (-\rho,\ p_\mathrm{r},\ p_\perp,\ p_\perp), \tag{2}$$

the field equations are obtained as

$$\rho = \frac{\left(1 - \mathrm{e}^{-2\mu}\right)}{r^2} + \frac{2\mu'\mathrm{e}^{-2\mu}}{r}, \tag{3}$$

$$p_\mathrm{r} = \frac{2\gamma'\mathrm{e}^{-2\mu}}{r} - \frac{\left(1 - \mathrm{e}^{-2\mu}\right)}{r^2}, \tag{4}$$

$$\Delta\mathrm{e}^{2\mu} = \gamma'' + \gamma'^2 - \gamma'\mu' - \frac{\gamma'}{r} - \frac{\mu'}{r} - \frac{\left(1 - \mathrm{e}^{2\mu}\right)}{r^2}, \tag{5}$$

where we have set $p_\perp - p_\mathrm{r} = \Delta$. In (3)–(5), ρ is the energy density, p_r is the radial pressure, $p_\perp$ is the tangential pressure and Δ is the measure of pressure anisotropy in this model. To solve this system we use the ansatz [22]

$$\mathrm{e}^{2\mu} = \frac{1 + \lambda r^2/R^2}{1 - r^2/R^2}, \ \Psi = \mathrm{e}^{\gamma(r)}, \ x^2 = 1 - \frac{r^2}{R^2}. \tag{6}$$

Then (5) takes the form

$$(1 + \lambda - \lambda x^2)\Psi_{xx} + \lambda x\Psi_x + \lambda(\lambda + 1)\Psi - \frac{\Delta R^2(1 + \lambda - \lambda x^2)^2}{(1 - x^2)}\Psi = 0. \tag{7}$$

To solve (7) we assume that the form of the anisotropic parameter Δ is

$$\Delta = \frac{\alpha \lambda^2 (1 - x^2)}{R^2 (1 + \lambda - \lambda x^2)^2},$$

and if we make a further transformation $z = \sqrt{\lambda/(\lambda + 1)}x$, (7) becomes

$$(1 - z^2)\Psi_{zz} + z\Psi_z + (\Lambda + 1)\Psi = 0, \tag{8}$$

where $\alpha = 1 - \Lambda/\lambda$ is a constant. This has the general solution (see [21] for details)

$$e^\gamma = A\left[\frac{\cos[(\beta + 1)\zeta + \delta]}{\beta + 1} - \frac{\cos[(\beta - 1)\zeta + \delta]}{\beta - 1}\right], \tag{9}$$

where $\beta = \sqrt{\Lambda + 2}$, $\zeta = \cos^{-1} z$, and A and δ are constants which can be determined from the boundary conditions. The physical parameters in this model are then obtained as

$$\rho = \frac{1}{R^2(1 - z^2)}\left[1 + \frac{2}{(\lambda + 1)(1 - z^2)}\right], \tag{10}$$

$$p_r = -\frac{1}{R^2(1 - z^2)}\left[1 + \frac{2z\Psi_z}{(\lambda + 1)\Psi}\right], \tag{11}$$

$$p_\perp = p_r + \Delta, \tag{12}$$

$$\Delta = \frac{\alpha\lambda}{R^2}\left[\frac{(\lambda + 1)(1 - z^2) - 1}{(\lambda + 1)^2(1 - z^2)^2}\right], \tag{13}$$

which together with (6) and (9) comprise an exact solution to the Einstein field equations. Note that

$$M(b) = \frac{(1 + \lambda)b^3}{2R^2(1 + \lambda\frac{b^2}{R^2})} \tag{14}$$

is the total mass of a star of radius b.

We impose the following conditions in our model:

- At the boundary of the star the interior solution should be matched with the Schwarzschild exterior solution, i.e.,

$$e^{2\gamma(r=b)} = e^{-2\mu(r=b)} = \left(1 - \frac{2M}{b}\right). \tag{15}$$

- The radial pressure p_r should vanish at the boundary of the star which gives

$$\frac{\Psi_z(z_b)}{\Psi(z_b)} = -\frac{(1 + \lambda)}{2z_b}, \tag{16}$$

where $z_b^2 = (\lambda/(\lambda+1))(1 - b^2/R^2)$. From (9) we have

$$\frac{\psi_z}{\psi} = \frac{(\beta^2 - 1)}{\sqrt{(1 - z^2)}} \left[\frac{\sin[(\beta - 1)\zeta + \delta] - \sin[(\beta + 1)\zeta + \delta]}{(\beta + 1)\cos[(\beta - 1)\zeta + \delta] - (\beta - 1)\cos[(\beta + 1)\zeta + \delta]} \right].$$

(17)

Combining (16) and (17) we obtain

$$\tan \delta = \frac{\tau \cot \zeta_b - \tan(\beta \zeta_b)}{1 + \tau \cot \zeta_b \tan(\beta \zeta_b)},$$

(18)

where $\tau = \frac{\lambda(1 - 2\alpha) + 1}{\beta(1 + \lambda)}$ and $\zeta_b = \cos^{-1} z_b$.

- $p_r \geq 0$ inside the star gives

$$\frac{\Psi_z}{\Psi} \leq -\frac{(1 + \lambda)}{2z}.$$

(19)

- Using (10)–(12) we get

$$\frac{\mathrm{d}p_r}{\mathrm{d}\rho} = \frac{z(1 - z^2)^2(\Psi_z/\Psi)^2 - (1 - z^2)\Psi_z/\Psi) - \alpha\lambda z(1 - z^2)}{z(1 - z^2)(1 + \lambda) + 4z},$$

(20)

$$\frac{\mathrm{d}p_\perp}{\mathrm{d}\rho} = \frac{\mathrm{d}p_r}{\mathrm{d}\rho} + \frac{\alpha\lambda}{(1 + \lambda)} \left[\frac{(\lambda + 1)(1 - z^2) - 2}{(\lambda + 1)(1 - z^2) + 4} \right].$$

(21)

We choose the parameters so that the causality conditions are not violated, i.e., $\mathrm{d}p_r/\mathrm{d}\rho, \mathrm{d}p_\perp/\mathrm{d}\rho \leq 1$ in this model.

The above conditions are imposed for a physically reasonable model.

3. Physical applications

It was shown earlier by Sharma *et al* [23] that the Vaidya–Tikekar model provides a simple method of studying systematically the maximum mass problem of compact isotropic ($\alpha = 0$) stars. To see the effect of anisotropy ($\alpha \neq 0$) in this model, we may adopt the following methods.

We may choose the isotropic compactness $u_i = (M/b)_{\mathrm{iso}}$ and λ as input parameters and using (14) calculate $y = b^2/R^2$. For a given central or surface density, (10) can be used to calculate the value of R which then determines the radius $b = R\sqrt{y}$ or mass M (from (14)). The parameter δ is fixed by choosing a specific value of α. Since mass and radius are fixed, this method is not suitable to analyze the role of anisotropy on the maximum mass problem. However, (20) and (21) can be utilized to show that stars with the same masses and radii may have different anisotropic compositions if the equations of state are modified accordingly. In §3.1, we consider two such examples to show how the composition may change in the presence of anisotropy. Note that the variations of the slopes of $\mathrm{d}p_r/\mathrm{d}\rho$ and $\mathrm{d}p_\perp/\mathrm{d}\rho$ may
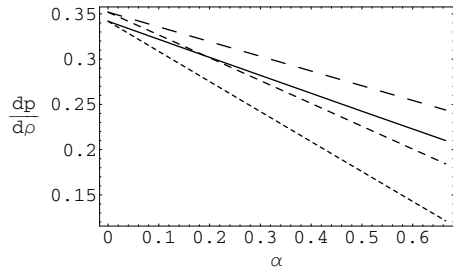
Figure 1. Variations of $dp/d\rho$ at the boundary and at the centre of an anisotropic star against α. We took $\lambda = 2$ and $u_i = 0.1686$. The solid line is for $(dp_r/d\rho)_{r=0}$, the dotted line is for $(dp_\perp/d\rho)_{r=0}$, the long dashed line is for $(dp_r/d\rho)_{r=b}$, and the dashed line is for $(dp_\perp/d\rho)_{r=b}$.
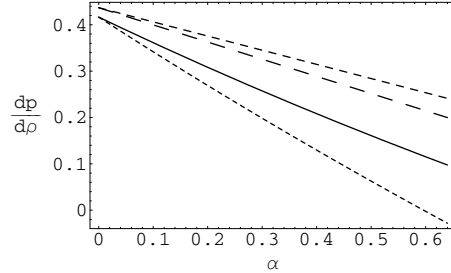
Figure 2. Variations of $dp/d\rho$ at the boundary and at the centre of an anisotropic star against α. We took $\lambda = 53.34$ and $u_i = 0.2994$. The solid line is for $(dp_r/d\rho)_{r=0}$, the dotted line is for $(dp_\perp/d\rho)_{r=0}$, the long dashed line is for $(dp_r/d\rho)_{r=b}$, and the dashed line is for $(dp_\perp/d\rho)_{r=b}$.

correspond to different material compositions within the star. These variations are shown in figures 1 and 2.

To see the effect of anisotropy on the compactness, we adopt a different approach. Note that (18) is a relation between y and δ which we will utilize to calculate δ for given values of α and λ. For given values of λ and u_i, we first calculate y using (14). Substituting these values in (18), we determine δ for the isotropic case ($\alpha = 0$). Once δ is determined, we use this value to calculate y_{ani} for different α values. We then use the relation

$$u_{\mathrm{ani}} = \frac{(1+\lambda)y_{\mathrm{ani}}}{2(1+\lambda y_{\mathrm{ani}})}$$

to see the effect of anisotropy on the compactness of a star.

3.1 *Numerical results*

Following the method discussed above, we have obtained numerical results showing the effect of anisotropy on some physically relevant parameters. Two different cases have been studied.

Case I: We use our earlier data for the pulsar Her X-1 [24] and choose $\lambda = 2$, $M = 0.88M_\odot$, $b = 7.7$ km so that $u_i = 0.1686$ and calculate the compactness for different anisotropic parameters.

Case II: We consider the millisecond pulsar SAX J 1808.4-3658 and use the results obtained in an earlier work [25] and choose $\lambda = 53.34$, $M = 1.435M_\odot$, $b = 7.07$ km so that $u_i = 0.2994$.

We note that the compactness decreases with increasing anisotropy which is in agreement with earlier results obtained in [17]. The results are shown in table 1.
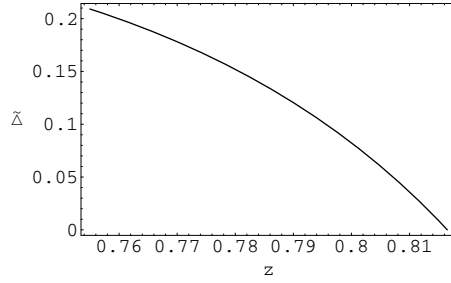
Figure 3. Variation of anisotropy factor ($\tilde{\Delta} = R^2\Delta$) against radial parameter z for $u_i = 0.1686$, $\lambda = 2$ and $\alpha = 0.6$.

Table 1. Compactness and mass calculated for different anisotropic parameters for two different cases discussed in §3.1.

$\lambda = 2$, $b = 7.7$ km				$\lambda = 53.34$, $b = 7.07$ km			
α	y_{ani}	u_{ani}	M_{ani} $(M_\odot)$	α	y_{ani}	u_{ani}	M_{ani} $(M_\odot)$
0	0.1450	0.1686	0.88	0	0.0267	0.2994	1.435
0.2	0.1281	0.1530	0.80	0.05	0.0269	0.3002	1.439
0.4	0.0953	0.1201	0.63	0.1	0.0270	0.3006	1.441
0.5	0.0690	0.0909	0.47	0.2	0.0268	0.2997	1.437
0.6	0.0322	0.0454	0.24	0.4	0.0239	0.2858	1.368
0.65	0.0082	0.0121	0.06	0.6	0.0090	0.1760	0.844

The behaviour of the anisotropy factor ($\tilde{\Delta} = R^2\Delta$) in the stellar interior is shown in figure 3.

4. Maximum mass and surface red-shift

In an earlier work [23], we calculated the maximum mass for a class of isotropic stars. Here we follow the same technique to calculate the maximum mass in the presence of pressure anisotropy.

- We assume that $\mathrm{d}p_{\mathrm{r}}/\mathrm{d}\rho \leq 1$ and the value is maximum at the centre. This gives

$$\frac{\psi_z}{\psi}\Big|_{zo} \geq \frac{(1+\lambda)}{2\sqrt{\lambda}}\left[\sqrt{\lambda+1} - \sqrt{21\lambda + 1 + \frac{4\alpha\lambda^2}{\lambda+1}}\right]. \tag{22}$$

Combining (17) and (22), we determine the limiting value of δ for different α values for a chosen value of λ.

- Corresponding to the limiting value of δ, (18) can be used to calculate the maximum value of $y = b^2/R^2$.

Table 2. Maximum compactness (u_{max}), maximum surface red-shift ($Z_s|_{\mathrm{max}}$) and maximum mass (M_{max}) for different anisotropic parameters. We have considered a star of radius 10 km and surface density equal to twice ρ_{nucl}, where, $\rho_{\mathrm{nucl}} = 2.7 \times 10^{14}$ gm/cm^3.

α	y_{max}	u_{max}	$Z_s|_{\mathrm{max}}$	$b = 10$ km M_{max} ($M_\odot$)	$\rho_b = 2\rho_{\mathrm{nucl}}$ M_{max} ($M_\odot$)	b_{max} (km)
0	0.0252	0.3615	0.9003	2.45	2.60	10.62
0.2	0.0285	0.3738	0.9910	2.53	2.69	10.62
0.4	0.0322	0.3852	1.0872	2.61	2.77	10.62
0.6	0.0361	0.3955	1.1879	2.68	2.84	10.62
0.7	0.0383	0.4003	1.2398	2.71	2.88	10.61
0.8	0.0404	0.4048	1.2927	2.74	2.91	10.60
0.9	0.0427	0.4092	1.3463	2.77	2.93	10.59
1.0	0.0450	0.4132	1.3998	2.80	2.96	10.58

- From (14) the compactness of a star in this model is given by

$$u = \frac{M(b)}{b} = \frac{(1+\lambda)}{2(\lambda + \frac{1}{y})}. \tag{23}$$

Clearly, the maximum value of y corresponds to the maximum compactness of the configuration. The maximum surface red-shift ($Z_s|_{\mathrm{max}}$) corresponding to this value can also be obtained using the following equation

$$Z_s|_{\mathrm{max}} = (1 - 2u_{\mathrm{ani}})^{-1/2} - 1. \tag{24}$$

Once the value of maximum compactness is obtained, the maximum mass of anisotropic star can be calculated for a given radius or surface density. In [23] we observed that for a particular choice ($\lambda = 100$), the maximum compactness for an isotropic star is 0.3615. Keeping the same value of λ if we go on increasing α we see that the maximum compactness, maximum surface red-shift and maximum mass all increase with anisotropy. The results are shown in table 2. For α close to unity (the maximum value of α in the present model is 1) these values are almost 0.4, 1.4 and 2.8$M_\odot$, respectively, for a star of radius 10 km. These values are similar to the results obtained in [26]. The maximum surface red-shift obtained by Bondi [27] was 1.352 which is also very close to our values. The maximum mass for an isotropic star of radius 10 km was 2.45$M_\odot$ [23], which increases to 2.8$M_\odot$ in the presence of anisotropy.

5. Discussion

We briefly point out the behaviour of the dynamical variables in this class of models. It is clear that the energy density ρ and the radial pressure p_{r} are decreasing
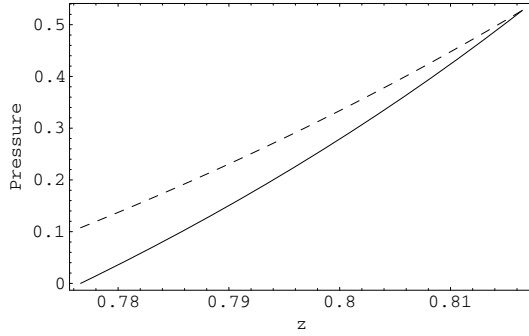
Figure 4. Radial pressure (solid curve) and tangential pressure (dashed curve) plotted against the radial parameter z for $\alpha = 0.4$ and $\lambda = 2$.

functions from the centre to the boundary of the star. This is also true for the anisotropic stellar models of Chaisi and Maharaj [19] and Sharma *et al* [25] who have studied the same space-time geometry. The tangential pressure $p_\perp$ has a more complicated behaviour because it is related to the anisotropy factor via $p_\perp = p_r + \Delta$; in addition $p_\perp$ depends on the Gegenbaur function and the new variable z rather than the original radial coordinate r. To illustrate the behaviour of $p_\perp$ we have generated a plot in figure 4. It is clear that the tangential pressure is an increasing function as we approach the centre. This is physically acceptable since the conservation of angular momentum during the quasi-equilibrium contraction of a massive body should lead to high values of $p_\perp$ in the central regions of the star.

We have extended a class of solutions describing cold compact stars to incorporate anisotropy. The solutions were then used to see the effect of anisotropy on the maximum possible mass and surface red-shift parameters of cold compact stars. A comparative study of our results with earlier results are given in table 3. The anisotropy in the present model vanishes at the centre and reaches the maximum value at the surface of the star as shown in figure 3. Unlike some earlier works [18,19], this model has an isotropic counterpart ($\alpha = 0$) which helps to compare anisotropic stars with their isotropic counterparts. In this model we assumed $p_\perp > p_r$ and have shown that the upper bound on the maximum mass increases in the presence of anisotropy. To conclude, our model provides a simple method to fix the

Table 3. Maximum compactness (u_{max}) and maximum surface red-shift ($Z_s|_{max}$) of anisotropic stars in different models.

References	$2u_{max}$	Zs_{max}
Guven and Murchadha [28]	0.974	5.211
Ivanov [29]	0.957	3.842
Bondi [27]	0.819	1.352
Hernández and Núñez [26]	0.800	1.200
Present work	0.826	1.400

upper bound on the maximum possible masses for the class of compact anisotropic stars described by the Vaidya–Tikekar model.

Acknowledgment

References

[1] E Witten, *Phys. Rev.* **D30**, 272 (1984)
[2] E Farhi and R L Jaffe, *Phys. Rev.* **D30**, 2379 (1984)
[3] Ch Kettner, F Weber, M K Weigel and N K Glendenning, *Phys. Rev.* **D51**, 1440 (1995)
[4] M Dey, I Bombaci, J Dey, S Ray and B C Samanta, *Phys. Lett.* **B438**, 123 (1998); Addendum: **447**, 352 (1999); Erratum: **467**, 303 (1999)
[5] J E Horvath and J A D F Pacheco, *Int. J. Mod. Phys.* **D7**, 19 (1998)
[6] V S U Maseswari, J N De and S K Samaddar, *Phys. Rev.* **D57**, 3242 (1998)
[7] R Ruffini and S Bonazzola, *Phys. Rev.* **187**, 1767 (1969)
[8] D J Kaup, *Phys. Rev.* **172**, 1331 (1968)
[9] M Colpi, S L Shapiro and I Wasserman, *Phys. Rev. Lett.* **57**, 2485 (1986)
[10] P Jetzer, *Phys. Rep.* **220**, 163 (1992)
[11] A B Henriques, A R Liddle and R G Moorhouse, *Nucl. Phys.* **B337**, 737 (1990)
[12] L Herrera and N O Santos, *Phys. Rep.* **286**, 53 (1997)
[13] R Tikekar and V O Thomas, *Pramana – J. Phys.* **52**, 237 (1999)
[14] L K Patel and N P Mehta, *Aust. J. Phys.* **48**, 635 (1995)
[15] S D Maharaj and R Maartens, *Gen. Relativ. Gravit.* **21**, 899 (1989)
[16] M K Gokhroo and A L Mehra, *Gen. Relativ. Gravit.* **26**, 75 (1994)
[17] M K Mak and T Harko, *Proc. R. Soc. London* **A459**, 393 (2003)
[18] K Dev and M Gleiser, *Int. J. Mod. Phys.* **D13**, 1389 (2004)
[19] M Chaisi and S D Maharaj, *Gen. Relativ. Gravit.* **37**, 1177 (2005)
[20] R L Bowers and E P T Liang, *Astrophys. J.* **188**, 657 (1974)
[21] S Mukherjee, B C Paul and N K Dadhich, *Class. Quantum Gravit.* **14**, 3475 (1997)
[22] P C Vaidya and R Tikekar, *J. Astrophys. Astron.* **3**, 325 (1982)
[23] R Sharma, S Mukherjee and S Karmakar, *Int. J. Mod. Phys.* **D15**, 405 (2006)
[24] R Sharma and S Mukherjee, *Mod. Phys. Lett.* **A16**, 1049 (2001)
[25] R Sharma, S Mukherjee, M Dey and J Dey, *Mod. Phys. Lett.* **A17**, 827 (2002)
[26] H Hernández and L A Núñez, *Can. J. Phys.* **82**, 29 (2004)
[27] H Bondi, *Mon. Not. R. Astron. Soc.* **259**, 365 (1992)
[28] J Guven and N O Murchadha, *Phys. Rev.* **D60**, 084020 (1999)
[29] B V Ivanov, *Phys. Rev.* **D65**, 104011 (2002)